Expanding the LISA Horizon from the Ground

Kaze W. K. Wong,[1,*] Ely D. Kovetz,[1,†] Curt Cutler,[2,3] and Emanuele Berti[1,4]
[1]*Department of Physics and Astronomy, Johns Hopkins University, Baltimore, Maryland 21218 USA*
[2]*Theoretical Astrophysics, California Institute of Technology, Pasadena, California 91125, USA*
[3]*Jet Propulsion Laboratory, 4800 Oak Grove Drive, Pasadena, California 91109, USA*
[4]*Department of Physics and Astronomy, The University of Mississippi, University, Mississippi 38677, USA*

(Received 28 August 2018; revised manuscript received 3 October 2018; published 17 December 2018)

The Laser Interferometer Space Antenna (LISA) gravitational-wave (GW) observatory will be limited in its ability to detect mergers of binary black holes (BBHs) in the stellar-mass range. A future ground-based detector network, meanwhile, will achieve by the LISA launch date a sensitivity that ensures complete detection of all mergers within a volume $> \mathcal{O}(10)$ Gpc^3. We propose a method to use the information from the ground to revisit the LISA data in search for subthreshold events. By discarding spurious triggers that do not overlap with the ground-based catalogue, we show that the signal-to-noise threshold $\rho_{\rm LISA}$ employed in LISA can be significantly lowered, greatly boosting the detection rate. The efficiency of this method depends predominantly on the rate of false-alarm increase when the threshold is lowered and on the uncertainty in the parameter estimation for the LISA events. As an example, we demonstrate that while all current LIGO BBH-merger detections would have evaded detection by LISA when employing a standard $\rho_{\rm LISA} = 8$ threshold, this method will allow us to easily (possibly) detect an event similar to GW150914 (GW170814) in LISA. Overall, we estimate that the total rate of stellar-mass BBH mergers detected by LISA can be boosted by a factor ~4 ($\gtrsim 8$) under conservative (optimistic) assumptions. This will enable new tests using multiband GW observations, significantly aided by the greatly increased lever arm in frequency.

DOI: 10.1103/PhysRevLett.121.251102

Multiband measurements of gravitational waves (GWs) [1] from coalescing binary black holes (BBHs) can open the door to a wide array of invaluable studies. Spanning a wider range of frequencies will increase sensitivity to eccentric orbits, which can be used to distinguish between different binary formation channels, improve merger-rate estimation, allow for more precise tests of gravity, and assist in instrument calibration. Better science will be enabled if many events are detected in both a ground-based network (ground) and a space observatory such as LISA.

Unfortunately, LISA will not be nearly as sensitive as the ground detectors to stellar-mass BBH mergers. This issue affects in particular multiband inspiral events, for which the GW frequency drifts from the LISA to the ground band during the LISA observation window. This condition determines a minimum frequency at which the event can appear in LISA (typically $\gtrsim 10^{-2}$ Hz for stellar-mass BBHs). Taking advanced LIGO (aLIGO) at design sensitivity as an example and adopting a similar signal-to-noise threshold of $\rho = 8$ in both experiments, the fraction of aLIGO events that will be detectable in LISA is less than 1%.

If we can manage to lower the LISA signal-to-noise threshold, the horizon distance (which is the maximum distance at which a source is detectable) will grow, and the increase in accessible volume will result in a rapid rise in the multiband detection rate. Setting a lower threshold, however, means that we increase the risk of classifying noise triggers as real events (false alarms). The false-alarm rate (FAR) is a steep function of ρ [2].

In this Letter we propose a method to discard spurious LISA triggers that show up as the signal-to-noise threshold is lowered, using information from the ground. We show that a large number of random noise triggers can be filtered out by imposing consistency with ground measurements for multiple parameters in tandem.

The procedure is as follows: we first set an initial threshold, e.g., $\rho_{\rm LISA} = 8$, and determine which (real) events in the ground catalogue are detectable in LISA with this threshold. The parameters of all LISA candidate events identified with this threshold are then compared with those in the ground list (taking into account the LISA parameter-estimation uncertainty), and those that do not overlap with any real event are discarded. We lower the threshold and iterate this procedure until the probability that a random trigger is consistent with some ground event becomes significant.

Figure 1 illustrates the concept of filtering spurious triggers using only t_c, the time of coalescence, as the discarding parameter. Compared with the entire LISA observation time, $\mathcal{O}(1)$ years, the typical uncertainty

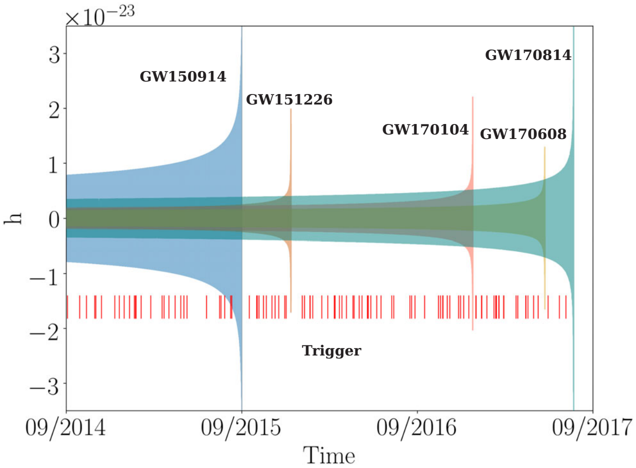

FIG. 1. Illustration of our method to discard LISA triggers. The waveforms are those of the gravitational events that were observed by aLIGO in its O1 and O2 runs (2015–2017). GW150914 would have had the highest signal to noise (SNR) in LISA, $\rho_{\rm LISA} = 7$, while GW170814 would have had $\rho_{\rm LISA} = 4.5$ (assuming 4 years of integration time), both of which are below the conventional $\rho = 8$ threshold. The red stripes indicate the merger time of LISA triggers (their width set by the uncertainty). If a trigger does not agree with any of the events detected from the ground, it can be discarded as random noise (or as an astrophysical event whose merger will appear in LIGO in the future and is thus irrelevant for our purposes). We show that if LISA had started observing in 2011, it would have been possible to lower its signal-to-noise threshold and recover GW150914, and potentially also GW170814. The other events would have been out of reach.

on t_c as determined by LISA is ~7 orders of magnitude smaller, $\mathcal{O}(10)$ seconds. With $\mathcal{O}(1000)$ events expected to be detected from the ground within the volume accessible by LISA with $\rho_{\rm LISA} \gtrsim 5$, we should therefore be able to filter out roughly $\gtrsim 10^4$ random triggers based on t_c alone. This allows a detection of events with $\rho_{\rm LISA} \sim 7$, such as GW150914 [3], over the LISA mission lifetime. We see that incorporating additional parameters may enable a multiband detection of events with $\rho_{\rm LISA} \sim 4$, such as GW170814 [4].

In what follows we choose to focus on three waveform ingredients: the source masses, sky location, and merger time. For simplicity we consider nonspinning, quasicircular BBHs. We test the efficiency of our proposed method based on a Fisher matrix analysis to estimate the parameter estimation uncertainty in the LISA band [5], and report the potential improvement in the LISA event rate given different assumptions about the FAR and the BBH mass function.

We assume the posteriors to be Gaussian, so a trigger is characterized by its k-dimensional vector of best-fit parameter values $\vec{\mu}$ and covariance matrix Σ. The problem of consistency checking between the LISA and ground measurements corresponds to finding the overlap between two volumes in a multidimensional space given some metric. We claim that two measurements taken by LISA and the ground agree with each other if they meet the following criterion:

$$D(\vec{\mu}_{\rm LISA}, \vec{\mu}_{\rm ground}, \Sigma_{\rm LISA}, \Sigma_{\rm ground}) \leq \chi_k^2(p), \tag{1}$$

where D is a function that gives the distance between two points in the high-dimensional space under some metric, and $\chi_k^2(p)$ is the quantile function for probability p of the chi-squared distribution with k degrees of freedom.

A typical source in LISA is characterized by $k = 9$ parameters (when taking into account the antenna pattern), so the exact two-point distance problem would be solved in an 18-dimensional space, and hence it can be computationally intensive. Instead of solving the problem exactly, we calculate the volume bounded by $\chi_k^2(p)$ in the parameter space centered at the best-fit value for each parameter that is given by the more precise measurement between the ground and LISA. Since most of the sources will be detected from the ground with signal to noise well above threshold, the ground measurements can be treated as the "true" values (neglecting any systematic bias). The consistent volume in parameter space of a particular source with parameters $\vec{\theta}$ is well approximated by the volume of a k-dimensional hyperellipsoid corresponding to a multivariate Gaussian distribution [6] with confidence level p,

$$V(\vec{\theta}, p) = \left(\frac{\chi_k^2(p)}{\chi_k^2(0.67)}\right)^k \sqrt{(2\pi)^k |\Sigma_{\rm LISA}(\vec{\theta})|}, \tag{2}$$

where $|\Sigma_{\rm LISA}(\vec{\theta})|$ denotes the determinant of the covariance matrix given by LISA using the most recent noise power spectral density $S_n(f)$ [7], and $\chi_k^2(0.67)$ corresponds to a bound at "1σ" level. We compute the volume using a 3σ cut, corresponding to $p = 0.997$. The fraction of triggers that are consistent between the two detectors is then given by

$$f_c(\rho, T) = \frac{\int d\vec{\theta} n_s(\vec{\theta}, \rho, T) \int_{V(\vec{\theta}, p)} d\vec{\theta}' n_b(\vec{\theta}')}{\int n_b(\vec{\theta}') d\vec{\theta}'}, \tag{3}$$

where $n_b(\vec{\theta}, \rho, T)$ is the number density of astrophysical (real) events that LISA is sensitive to (all of which are detectable from the ground) for a given vector $\vec{\theta}$ of source parameters, a signal-to-noise threshold $\rho_{\rm LISA}$, and integration time T; $n_b(\vec{\theta}')$ is the number density of LISA triggers as a function of $\vec{\theta}'$ in the search parameter space.

The most important ingredient in our analysis is the relationship between the threshold $\rho_{\rm LISA}$ and the number of expected background triggers, which we call the "FAR curve." At this time, there is no reliable estimate for the LISA FAR curve. We therefore use as a proxy the results of the LIGO Mock Data Challenge [2], which suggest that the number of background triggers increases by about 2 orders of magnitude when the signal-to-noise threshold is decreased by 1 (we use their experiment 3, which is the most relevant for our study). This agrees with the recent findings of Ref. [8].

We can then define the *effective* LISA threshold as

$$\rho_{\rm LISA}^{\rm eff}(T) = \rho_{\rm LISA}^{0} + \log_{\Gamma}[f_c(\rho_{\rm LISA}^{\rm eff}, T)], \qquad (4)$$

where $\rho_{\rm LISA}^{0}$ is the conventional signal-to-noise threshold, Γ is the rate of change in the number of background triggers as a function of the SNR threshold, and T is the integration time in LISA. Equation (4) is the crux of the method proposed in this work, and we denote this as FAR curve henceforth.

The FAR curve given in Ref. [2] has a slope $\Gamma \sim 100$ above $\rho = 5.5$, and it is not shown below $\rho = 5.5$. As a conservative estimate, we impose an exponential cutoff $e^{-3(\rho-5.5)}$ starting at $\rho = 5.5$, essentially preventing any improvement beyond $\rho = 5$. We also consider a more optimistic case in which we extrapolate the FAR curve with a similar cutoff at $\rho = 4$. Given the volume permitted by a single source, Eq. (2), the number density n_s of real sources in the parameter space and the FAR function, we are now ready to obtain $\rho_{\rm eff}$ by solving Eq. (4) self-consistently.

In order to compute the second integral in Eq. (3), we need to estimate $\Sigma_{\rm LISA}$. We adopt a modification of the Fisher matrix code from Ref. [5] to calculate the uncertainties on source parameters. As explained above, we calculate $\rho_{\rm LISA}^{\rm eff}(T)$ using the three groups of parameters that minimize the fraction of coincident events f_c.

(i) Time of coalescence t_c: we care only for events that merge in the ground frequency band and assume that noise triggers will be distributed uniformly in the LISA observation window, which is determined by T.

(ii) Component masses (M_1, M_2): we assume that noise triggers will pick up a random template in the template bank, and calculate the fraction f_c assuming noise triggers are distributed uniformly in the (M_1, M_2) plane. The uncertainty on either component mass is normally ~10% of the measured value, but due to the strong correlation between the two component masses [9], the allowed volume in the parameter space is typically much smaller than 10%. This volume is related to the uncertainty in chirp mass measurement, which is expected to be quite small in LISA (as BBHs spend many cycles in its frequency band). Typically the probability of a noise trigger being consistent with one real event is $\sim 10^{-6}$.

(iii) Sky location (θ_S, ϕ_S): We assume that noise triggers will be uniformly distributed across the sky. LISA will be able to localize sources to within $\mathcal{O}(10)$ deg^2 [10]. Comparing to the whole sky, the probability of a noise trigger being consistent with one event is $\lesssim 10^{-3}$.

Our figure of merit is the number of additional sources we can recover in LISA by replacing the conventional threshold $\rho_{\rm LISA}^{0}$ with $\rho_{\rm LISA}^{\rm eff}$. This of course depends on the astrophysical BBH merger rate. Multiband events probed by LISA are in the local Universe, so we can assume the merger-rate density R to be constant in redshift. We denote by Λ the mean rate of events of astrophysical origin above a certain signal-to-noise threshold, given by $\Lambda = R\langle VT\rangle$, where $\langle VT\rangle f$ is the time and population-averaged space-time volume accessible to the detector at the chosen threshold $\rho^{\rm th}$, defined as [11]

$$\langle VT\rangle = T\int dz d\vec{\theta}\frac{dV_c}{dz}\frac{1}{1+z}s(\vec{\theta})f(z,\vec{\theta},\rho^{\rm th}), \qquad (5)$$

where V_c is the comoving volume, $s(\vec{\theta})$ is the injected distribution of source parameters, and $0 \le f(z,\vec{\theta},\rho^{\rm th}) \le 1$ is the fraction of injections detectable by the experiment.

In order to calculate $\langle VT\rangle$, we need to solve for the horizon distance and redshifted volume as a function of source parameters [12], and then marginalize over an input population $s(\vec{\theta})$. We consider sources characterized by nine parameters: the two component masses (M_1, M_2), time of coalescence t_c, phase of coalescence ϕ_c, luminosity distance D_L, sky locations of the source $(\bar{\theta}_S, \bar{\phi}_S)$, and the orbital angular momentum direction $(\bar{\theta}_L, \bar{\phi}_L)$. In practice, we sample over the two component masses and four sky locations, with t_c and ϕ_c arbitrarily set to 0.

For the injected mass distribution, we follow Ref. [13] and define the probability density function (PDF) of M_1,

$$P(M_1) \equiv A_{M_1}M_1{}^{-\alpha}\mathcal{H}(M_1 - M_{\rm gap})e^{-(M_1/M_{\rm cut})^2}, \qquad (6)$$

where A_{M_1} is a normalization constant, $\mathcal{H}$ is the Heaviside function, $M_{\rm gap}$ is the minimum mass of a stellar black hole (assumed to be 5 $M_\odot$), and by default we set the upper cutoff $M_{\rm cut} = 40\ M_\odot$ [14–16]. To account for uncertainty regarding these choices, we also calculate our results using two other mass functions: in one we replace the Gaussian cutoff with a sharp step function $P(M) \propto \mathcal{H}(M_\odot - M_{\rm cut})$, and in another with an exponential cutoff $P(M) \propto e^{-M_1/M_{\rm cut}}$. For all cases we limit the maximum component mass to 100 $M_\odot$. Finally, given a value for M_1, we define the PDF of M_2 as a uniform distribution ranging from $M_{\rm gap}$ to M_1 [9,13],

$$P(M_2|M_1) \equiv A_{M_2}\mathcal{H}(M_2 - M_{\rm gap})\mathcal{H}(M_1 - M_2). \qquad (7)$$

We assume a uniform comoving volume merger-rate density R, so the distribution of the luminosity distance D_L follows from the functional form of the comoving volume. We assume isotropic distributions for the position of the source in the sky and for the direction of the orbital angular momentum. In principle, one should generate a six-dimensional sample in the mass-sky-location parameters space, but this is quite computationally intensive. In practice, we average over a reasonable amount of sources distributed across the sky and compress the calculation of $\langle VT \rangle$ to two (mass) dimensions.

The next term we need is $f(z, \vec{\theta}, \rho^{\rm th})$, which is related to the horizon redshift of the source. The LISA signal to noise of a source with frequency-domain waveform $\tilde{h}(f)$ at some luminosity distance is given by [17]

$$\rho^2 = 4 \int_{f_{\rm min}}^{f_{\rm max}} \frac{\tilde{h}^*(f)\tilde{h}(f)}{S_n(f)} df, \tag{8}$$

where $f_{\rm min}$ and $f_{\rm max}$ are the initial and final frequencies. We get the horizon redshift, and hence $f(z, \vec{\theta}, \rho^{\rm th})$, by setting $\rho = \rho^{\rm th}$.

When calculating the uncertainty and signal to noise for a given source, we need to integrate the waveform over a certain frequency range. Since we are interested in sources that can in principle be detected in both LISA and the ground, we set $f_{\rm max} = 1$ Hz (the conventional upper cutoff on the LISA noise curve). To determine $f_{\rm min}$, we require that a source drifts from the LISA band to the ground band in less than a total time T. The chirp time of a source with chirp mass $\mathcal{M}$ (in the observer frame) is given by [18]

$$t = \int_{f_{\rm min}}^{f_{\rm max}} df \frac{5c^5}{96\pi^{8/3}} (G\mathcal{M})^{-5/3} f^{-11/3}. \tag{9}$$

To determine $f_{\rm min}(\vec{\theta})$ we solve Eq. (9) setting $t \equiv T$.

In Fig. 2 we plot our main result: $\Lambda_{\rho_{\rm eff}}/\Lambda_{\rho=8}$, the increase in detection rate compared to using the standard $\rho = 8$ threshold, under different assumptions. We see that using the ground information can boost the number of detections in LISA by a factor ~4, under the conservative choice for the FAR.

Since our figure of merit compares total rates, and we assume a constant merger-rate density per comoving volume, the uncertainties in the merger rate cancel out. The dominant uncertainty in our result stems from the FAR. With a more optimistic choice of FAR the boost factor can increase up to ~8: the LISA sampling rate [19] sets a lower limit on the threshold.

The next source of uncertainty is due to the choice of mass function. The increase in detection rate is biased toward the lower end of the mass function, and so it is more significant for mass functions that favor lower mass events. This uncertainty amounts to ~5%. A uniform-in-log mass function should yield similar results [8].

Various assumptions we have made here can be improved upon. For example, in checking for consistency between LISA and the ground we considered only the volume allowed by the LISA covariance matrix, instead of solving the exact two-point problem. This is a reasonable

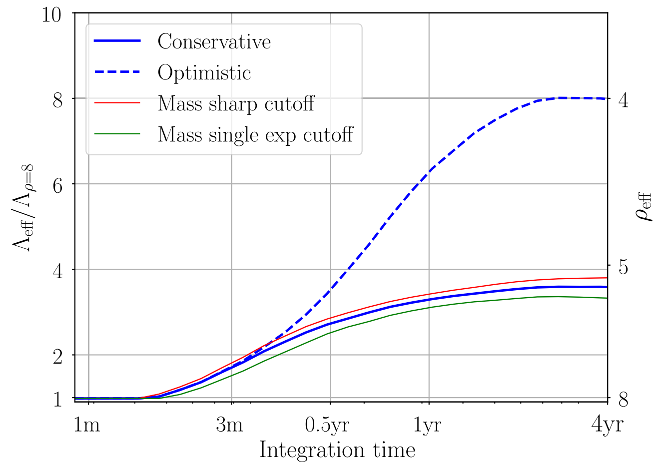

FIG. 2. The boost in the LISA detection rate enabled by our method, compared to setting the standard signal-to-noise threshold of $\rho = 8$, and assuming that all sources are observed for the integration time T given in Eq. (9). The blue solid line shows the rate increase using a FAR function with a cutoff at $\rho = 5$ and a mass function with a Gaussian cutoff. The dashed-blue line corresponds to a more optimistic FAR function, where the cutoff is at $\rho = 4$. For comparison, we show in red and green the result when using a mass function with a sharp cutoff at 50 $M_\odot$ and a single-exponential cutoff at 40 $M_\odot$, respectively.

assumption, based on the expected sensitivity of ground observatories by the time LISA flies.

We also took the distribution of noise triggers to be uniform in the parameters of interest. This assumption is valid for time of coalescence and sky location, but it may not be accurate for the two component masses. Search template banks for ground-based detectors typically have more templates at the low-mass end [20–22]. More realistic template banks for LISA, when available, can be used to replace the uniform distribution employed here. If the LISA and ground templates are qualitatively similar, this replacement should increase the discarding power at the higher-mass end compared to the uniform case, and therefore improve the boost in rate.

Another approximation we made was to extrapolate our Fisher matrix calculation into the low signal-to-noise regime, where it generally serves only as a lower bound of the uncertainties [23]. A more accurate estimate of the uncertainties can be achieved with other parameter-estimation approaches, such as the Markov chain Monte Carlo method [24]. We hope that our work will motivate participants in the ongoing LISA Data Challenges [25] to verify and improve our FAR estimates.

To conclude, while the idea to use LISA detections to alert ground-based experiments about pending mergers has been explored before [1], we have investigated for the first time the potential of exploiting the opposite route.

We have introduced in this Letter a method to recover subthreshold stellar-mass BBH merger events from the LISA data stream using information from the subsequent ground-based measurements of these events. Our analysis forecasts a remarkable increase—by a factor of 4 to 8, depending on the assumptions—in the number of LISA detections. While our estimate was restricted to multiband sources whose merger is detected from the ground during the LISA lifetime, the same algorithm can be continuously applied for events that merge after LISA has finished its mission, yielding more detections. It is also worth mentioning that by the time LISA flies, third-generation detectors such as the Einstein Telescope [26,27] or Cosmic Explorer [28] may be taking data. Compared to Advanced LIGO, these detectors will observe events with much higher SNRs and lower parameter-estimation uncertainties, further improving the efficiency of our proposed method and the resulting science.

The increase in number of multiband GW detections can bring forth a plethora of rewards. LISA and LIGO measurements will be made in different frequency bands and target different physical observables, possibly breaking degeneracies. For example, even a low-SNR LISA detection could measure the chirp mass reasonably well, while a ground detection could determine the total mass of the remnant. Furthermore, if even a small fraction of the "extra" binaries detectable by our method were to be eccentric, this may have very significant implications for population studies, allowing us to discriminate between different BBH formation channels [29–36]. This could also be accomplished by measuring spins [37–41] and other waveform features [42–44]. Improvements in parameter estimation and modeling constraints may also enable novel tests of gravity in the strong-field regime [45–49].

It is our pleasure to thank Ilias Cholis, Marc Kamionkowski, Johan Samsing, and Fabian Schmidt for useful discussions. K. W. K. W. and E. B. are supported by NSF Grants No. PHY-1841464, No. AST-1841358, and NASA ATP Grant No. 17-ATP17-0225. E. D. K. was supported by NASA Grant No. NNX17AK38G. C. C.'s work was carried out at the Jet Propulsion Laboratory, California Institute of Technology, under contract to the National Aeronautics and Space Administration. C. C. also gratefully acknowledges support from NSF Grant No. PHY-1708212.

[*]kazewong@jhu.edu
[†]ekovetz1@jhu.edu

[1] A. Sesana, Phys. Rev. Lett. **116**, 231102 (2016).
[2] C. Capano, T. Dent, C. Hanna, M. Hendry, Y.-M. Hu, C. Messenger, and J. Veitch, Phys. Rev. D **96**, 082002 (2017).
[3] B. P. Abbott *et al.* (Virgo and LIGO Scientific Collaborations), Phys. Rev. Lett. **116**, 061102 (2016).
[4] B. P. Abbott *et al.* (Virgo and LIGO Scientific Collaborations), Astrophys. J. **851**, L35 (2017).
[5] E. Berti, A. Buonanno,, and C. M. Will, Phys. Rev. D **71**, 084025 (2005).
[6] P. Gregory, *Bayesian Logical Data Analysis for the Physical Sciences*, edited by P. Gregory (Cambridge University Press, Cambridge, England, 2010).
[7] N. Cornish and T. Robson, arXiv:1803.01944.
[8] R. Lynch, M. Coughlin, S. Vitale, C. W. Stubbs, and E. Katsavounidis, Astrophys. J. **861**, L24 (2018).
[9] B. P. Abbott *et al.* (Virgo and LIGO Scientific Collaborations), Phys. Rev. X **6**, 041015 (2016).
[10] W. Del Pozzo, A. Sesana, and A. Klein, Mon. Not. R. Astron. Soc. **475**, 3485 (2018).
[11] B. P. Abbott *et al.* (Virgo and LIGO Scientific Collaborations), Astrophys. J. **833**, L1 (2016).
[12] H.-Y. Chen, D. E. Holz, J. Miller, M. Evans, S. Vitale, and J. Creighton, arXiv:1709.08079.
[13] E. D. Kovetz, I. Cholis, P. C. Breysse, and M. Kamionkowski, Phys. Rev. D **95**, 103010 (2017).
[14] K. Belczynski *et al.*, Astron. Astrophys. **594**, A97 (2016).
[15] M. Fishbach and D. E. Holz, Astrophys. J. **851**, L25 (2017).
[16] E. D. Kovetz, I. Cholis, M. Kamionkowski, and J. Silk, Phys. Rev. D **97**, 123003 (2018).
[17] E. E. Flanagan and S. A. Hughes, Phys. Rev. D **57**, 4535 (1998).
[18] C. Cutler and E. E. Flanagan, Phys. Rev. D **49**, 2658 (1994).
[19] H. Audley *et al.* (LISA Collaboration), arXiv:1702.00786.
[20] T. Dal Canton *et al.*, Phys. Rev. D **90**, 082004 (2014).
[21] S. A. Usman *et al.*, Classical Quantum Gravity **33**, 215004 (2016).
[22] A. H. Nitz, T. Dent, T. Dal Canton, S. Fairhurst, and D. A. Brown, Astrophys. J. **849**, 118 (2017).
[23] M. Vallisneri, Phys. Rev. D **77**, 042001 (2008).
[24] M. van der Sluys, V. Raymond, I. Mandel, C. Rover, N. Christensen, V. Kalogera, R. Meyer, and A. Vecchio, Classical Quantum Gravity **25**, 184011 (2008).
[25] https://lisa-ldc.lal.in2p3.fr/.
[26] M. Punturo *et al.*, Classical Quantum Gravity **27**, 194002 (2010).
[27] B. Sathyaprakash *et al.*, *Gravitational Waves and Experimental Gravity*, edited by E. Auge, J. Dumarchez, and J. Thanh Tran Van (The Gioi Publishers, , Vietnam, 2011), pp. 127–136.
[28] B.P. Abbott *et al.* (LIGO Scientific Collaboration), Classical Quantum Gravity **34**, 044001 (2017).
[29] I. Cholis, E.D. Kovetz, Y. Ali-Haïmoud, S. Bird, M. Kamionkowski, J.B. Muñoz, and A. Raccanelli, Phys. Rev. D **94**, 084013 (2016).
[30] A. Nishizawa, E. Berti, A. Klein, and A. Sesana, Phys. Rev. D **94**, 064020 (2016).
[31] K. Breivik, C. L. Rodriguez, S. L. Larson, V. Kalogera, and F. A. Rasio, Astrophys. J. **830**, L18 (2016).
[32] A. Nishizawa, A. Sesana, E. Berti, and A. Klein, Mon. Not. R. Astron. Soc. **465**, 4375 (2017).
[33] L. Gondán, B. Kocsis, P. Raffai, and Z. Frei, Astrophys. J. **855**, 34 (2018).
[34] D. J. D'Orazio and J. Samsing, Mon. Not. R. Astron. Soc. **481**, 4775 (2018).
[35] J. Samsing and D. J. D'Orazio, Mon. Not. R. Astron. Soc. **481**, 5445 (2018).
[36] J. Samsing and D. J. D'Orazio, arXiv:1807.08864.

[37] S. Vitale, R. Lynch, R. Sturani, and P. Graff, Classical Quantum Gravity **34**, 03LT01 (2017).
[38] C. L. Rodriguez, M. Zevin, C. Pankow, V. Kalogera, and F. A. Rasio, Astrophys. J. **832**, L2 (2016).
[39] D. Gerosa and E. Berti, Phys. Rev. D **95**, 124046 (2017).
[40] S. Stevenson, C. P. L. Berry, and I. Mandel, Mon. Not. R. Astron. Soc. **471**, 2801 (2017).
[41] D. Gerosa, E. Berti, R. O'Shaughnessy, K. Belczynski, M. Kesden, D. Wysocki, and W. Gladysz, Phys. Rev. D **98**, 084036 (2018).
[42] K. Inayoshi, N. Tamanini, C. Caprini, and Z. Haiman, Phys. Rev. D **96**, 063014 (2017).
[43] K. Kremer, S. Chatterjee, K. Breivik, C. L. Rodriguez, S. L. Larson, and F. A. Rasio, Phys. Rev. Lett. **120**, 191103 (2018).
[44] J. Samsing, D. J. D'Orazio, A. Askar, and M. Giersz, arXiv:1802.08654.
[45] M. Agathos, W. Del Pozzo, T. G. F. Li, C. Van Den Broeck, J. Veitch, and S. Vitale, Phys. Rev. D **89**, 082001 (2014).
[46] B. P. Abbott *et al.* (Virgo and LIGO Scientific Collaborations), Phys. Rev. Lett. **116**, 221101 (2016).
[47] S. Vitale, Phys. Rev. Lett. **117**, 051102 (2016).
[48] E. Barausse, N. Yunes, and K. Chamberlain, Phys. Rev. Lett. **116**, 241104 (2016).
[49] N. Yunes, K. Yagi, and F. Pretorius, Phys. Rev. D **94**, 084002 (2016).